PROCEEDINGS OF SCIENCE

Electric Field Induced Lyman-α Emission (EFILE) Diagnostic For Electric Field Measurements

Laurence Chérigier-Kovacic[*†]
Aix-Marseille Université, CNRS, PIIM UMR 7345, FR-13397 Marseille cedex 20, France
E-mail: laurence.kovacic@univ-amu.fr

Petter Ström
Department of Fusion Plasma Physics, Royal Institute of Technology (KTH), Teknikringen 31, 100 44 Stockholm, Sweden
E-mail: pestro@kth.se

Fabrice Doveil
Aix-Marseille Université, CNRS, PIIM UMR 7345, FR-13397 Marseille cedex 20, France
E-mail: fabrice.doveil@univ-amu.fr

When a metastable hydrogen test beam is exposed to a constant or oscillating electric field, Lyman-α (121.6 nm) emission occurs. This results from the Stark quenching of the metastable $2s$ level, induced by the field. The intensity of the radiation is proportional to the square of the electric field amplitude and it is recorded by a lock-in technique, which gives an excellent signal to noise ratio. This provides us with a very sensitive and non intrusive method to measure the electric field value, called EFILE (Electric Field Induced Lyman-α emission). Sensitivity is as good as 0.1 V/cm in the case of an oscillatory field resonant with the Lamb shift frequency ≈ 1 GHz.

Hydrogen ions are produced in a magnetic multicusp source by a thermo-electronic discharge. The ions are extracted from the source, focused by a series of electrostatic lenses and accelerated to 500 eV. The beam interacts with cesium vapor which produces atoms in the metastable $2s_{1/2}$ state. In the diagnosed volume, the beam passes between a pair of plane electrodes separated by 5 cm. One of them is grounded, the other one is polarized to generate an electric field. The diagnosed volume can be kept under vacuum or exposed to an argon plasma.

Lyman-α emission from the beam passing between the plates is measured as a function of the polarized plate voltage. A saturation of the signal is observed at large field amplitudes, which is explained through oscillatory and geometrical mechanisms. A function that takes this saturation into account is used as a calibration for the subsequent electric field profile measurements in the case of a constant voltage applied between the plates in vacuum. We find a good agreement between our results and a finite element method calculation of the profile.

1st EPS conference on Plasma Diagnostics
14-17 April 2015
Frascati, Italy

[*]Speaker.
[†]A footnote may follow.

PoS(ECPD2015)124

1. Theoretical background

In hydrogen atoms and hydrogen-like ions, as initially discovered by Lamb *et al.* in the late forties and early fifties, the excited state $2s_{1/2}$ lies higher than $2p_{1/2}$ by $\varepsilon \approx 4.4 \cdot 10^{-6}$ eV (Lamb-shift)[1]. Oscillations between $2s_{1/2}$ and $2p_{1/2}$ are caused by interaction with the electric field (Stark mixing), inducing a transition to the ground state with emission of a Lyman-α radiation at a wavelength of 121.6 nm.

The transition rate is calculated by solving the time-dependent Schrödinger equation [2]. The electric field is treated as a perturbation of the Hamiltonian of the hydrogen atoms, and only the two states of interest are considered. Transitions to the ground state are taken into account by assuming a fixed decay rate for $2p_{1/2}$. In the case of a static field, as long as its magnitude is lower than 260 V/cm, the problem can be solved analytically. Calling $\gamma_{2\mathrm{p}}$ the decay rate of the $2p$ state, $\hbar\omega_L$ the energy difference associated to the Lamb-shift ($\nu_L = 1057$ MHz), e the elementary charge and a_0 the Bohr radius, one gets the quenched $2s$ level decay rate:

$$\gamma_{2s}^{*} = \frac{9e^2a_0^2E^2}{\hbar^2}\frac{\gamma_{2p}}{\omega_L^2 + \gamma_{2p}^2/4} \tag{1.1}$$

Since the intensity of the Lyman-α radiation is proportional to γ_{2s}^{*}, it is possible to measure the perturbing field.

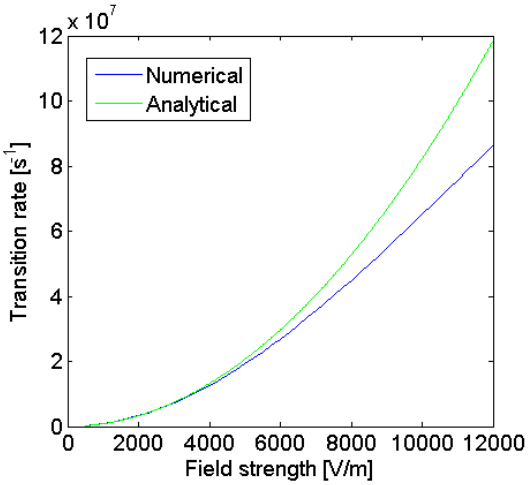

Figure 1.1 – Transition rates to the ground state, numerically and analytically obtained. The figure shows that oscillatory saturation takes effect at low field strengths.

For larger field strengths, though, the analytical solution starts to become inaccurate and we solve the system of equations that arise from the Schrödinger equation numerically. Fig. 1.1 shows the field strength dependence of the resulting rate compared to the one given by (1.1). It is clear that the numerical result agrees with the analytical one in the weak field limit, but for stronger fields it shows saturation which is not accounted for in the analytical solution. If the oscillations between $2s_{1/2}$ and $2p_{1/2}$ occur on a time scale that is faster than the rate at which $2p_{1/2}$ decays to the ground state, increasing the field strength further won't increase the transition rate to the ground state, and saturation occurs.

This *oscillatory saturation* is thus related to the field strength dependent ratio between the finite lifetime of the $2p_{1/2}$ and the period time of Stark mixing oscillations. The oscillatory mechanism has been examined in order to find out how strongly it affects the experimental results. As presented later on in this paper, there is at least one other mechanism that contributes to the saturation of the signal at high field strengths, due to a geometrical feature of our experiment.

2. Experimental set-up

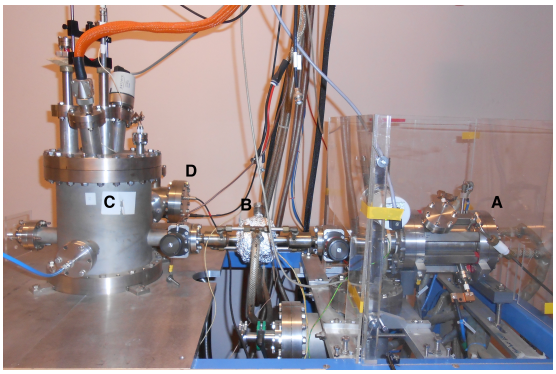

Figure 2.1 – Photograph of our experiment with component designations

A thermionic discharge is created in a cylindrical vessel filled with hydrogen gas [3]. An ion beam containing H^+ is extracted at a frequency of 1 Hz and a 500 eV energy from the source (labelled A in Fig. 2.1). The beam is focused into a heated cesium cell (B) where protons undergo a charge exchange process and become metastable atoms H(2*s*)[4]. Then the beam enters the measurement chamber (C) and passes between two plates, 5 cm apart. The upper plate is grounded and the lower plate can be biased either positively or negatively to create an electric field.

Emitted Lyman-α radiation is detected using a photomultiplier behind an optical filter (D) with a lock-in amplifier synchronized with the pulsed ion beam to distinguish the part of the measured signal that is due to the beam from background. A Faraday cup is used to measure the ion content of the beam. In addition, there is a filament in the measurement chamber which makes it possible to generate a plasma by the same method as in the source.

3. Field measurements in vacuum : strong field saturation

The theoretical E^2-dependence of the transition rate to the ground state has first been tested in the simple case of a static electric field in vacuum.

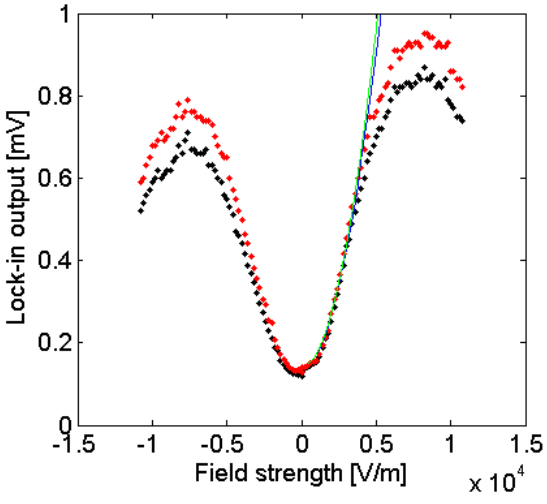

Figure 3.1 – Electric field strength dependence measurement, raw data, coated plates.

A typical resulting lock-in output is given in Fig. 3.1 with the x-axis scaled in volts per meter. This scale is obtained by assuming a homogeneous field between the plates. The output of our experiments oscillates between the upper and the lower set of points because of temperature variations due to the slow response time of the regulator used with the cesium cell heater. The two overlaid curves in Fig. 3.1 are the analytical result by expression (1.1) (upper, green) and the numerical result of Fig. 1.1 (lower, blue) both scaled by a factor of $4 \cdot 10^{-8}$ and shifted upwards by the positive branch 0-field offset of 0.141mV. The E^2-dependence predicted by (1.1) is verified in the weak field limit.

We note though, that strong field saturation occurs much earlier than the numerical treatment suggests. Oscillatory saturation does not have a significant impact at these field strengths, so we

conclude that another saturation mechanism is at work. The asymmetry in the saturation is, just like the discontinuity at 0V, explained by charge accumulation on the insulated parts of the plate assembly. In Fig. 3.1, both plates are covered by a ceramic coating, only exposing a rectangular area of 1.5×8 cm at the center. This measure was taken with the intent of trying to make the electric field more homogenous and localized in space than if the plates had simply been bare. The effect has been verified, but because the coating also increased problems with charge accumulation, it was later removed. Indeed, the same curve in the case of bare plates is more symmetrical than in the previous case, indicating less influence of charging.

We explain the strong saturation by assuming that the field in the measurement chamber is not localized to the region from which emitted radiation is collected. By interacting with the field before reaching the measurement region, much of the 2s hydrogen can decay without it being detected, thereby saturating the signal before the theoretically predicted limit.

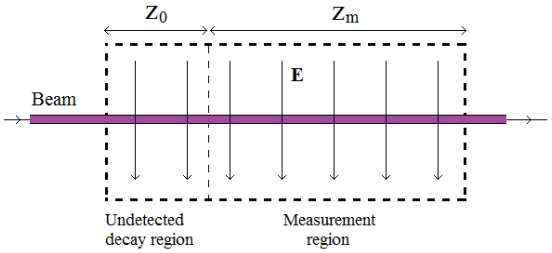

Figure 3.2 – Sketch of the cause of geometrical saturation

This mechanism is here referred to as *geometrical saturation*, and Fig. 3.2 shows a sketch of the idea. Parameters z_m and z_0 denote the lengths of the two regions and we have z_m=1 cm.
The number of particles that are left not decayed in the beam is $n_1 = n_0 e^{-\gamma z_0/v_b}$ and the number left after also passing the measurement region is $n_2 = n_0 e^{-\gamma(z_0+z_m)/v_b}$ where v_b is the speed of the hydrogen atoms in the beam.

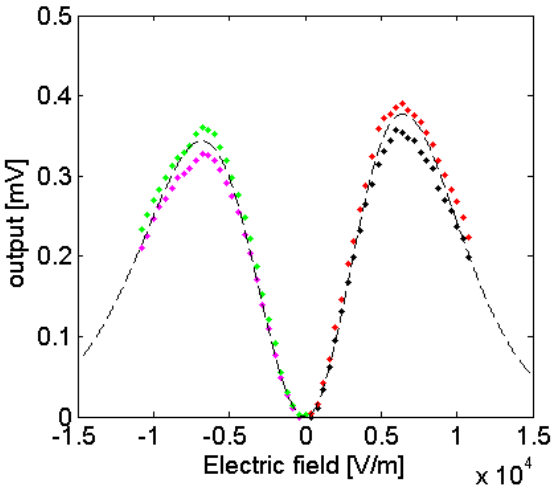

Figure 3.3 – Electric field strength dependence measurement, background subtracted, bare plates.

As geometrical saturation dominates over oscillatory saturation, γ can safely be approximated as correctly described by the theoretical rate of expression (1.1). The output, S, is assumed to depend linearly on the number of decays in the measurement region, giving the expression $S = S_0'(n_1 - n_2)$. Finally,

$$S(E) = S_0 e^{-\sigma A E^2}(1 - e^{-A E^2}) \qquad (3.1)$$

where $\sigma = z_0/z_m$ and in the case of a static field in vacuum, $A \approx 2.6617 \cdot 10^{-8} \left(\frac{\mathrm{V}}{\mathrm{m}}\right)^{-2}$. The continuous curve in Fig. 3.3 shows the result of fitting (3.1) to the data by adjusting parameters S_0 and σ and serves as calibration function for profile measurements.

The length of the undetected decay region, z_0, turns out to be about 0.5 mm. This is almost twice as long as with coated plates (the value of σ is almost doubled) and verifies the original intent of adding the coating, namely to localize the electric field to the measurement region. But as the problem with charging is expected to increase dramatically in a plasma, the benefits of the coating

have, on the basis of data obtained for static fields in vacuum, been concluded to be too small to make up for the disadvantages.

4. Field profile between the plates

We have recorded the electric field profile between the bare plates by moving them vertically with respect to the beam and measuring the lock-in output at up to 28 points (Fig. 4.1). This has been done for several static voltage settings from 0 V to + 500 V in vacuum. The points around 5 cm correspond to the beam passing very close to the upper (grounded) plate, and the points at 10 cm give the same for the lower (biased) plate.

The raw field profile graphs shown in Fig. 4.1 are affected by geometrical saturation as well as the influence of the plates. Both effects should be compensated for in order to reconstruct the electric field profiles. The influence of the plates is taken care of first by renormalizing the 0-field profile so that its average value between the plates is unity. All data is then divided by this renormalized profile, point by point, rescaling data close to the plates in a manner inverse to the effects of plate influence. The constant 0-field profile is then subtracted from all data. The resulting curves are compared to the saturation function obtained in section 3 in order to account for geometrical saturation and get back the electric field. We first assume a homogenous field in order to relate the calibration curve to an electric field scale in the case where the beam is centered between the plates, and then we apply the result as a calibration for all collected data. As a consequence we consider the geometrical saturation to occur with the same value of z_0 for all plate positions.

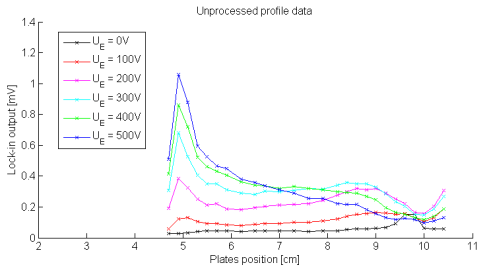

Figure 4.1 – Raw data of profile measurements in vacuum, static field case.

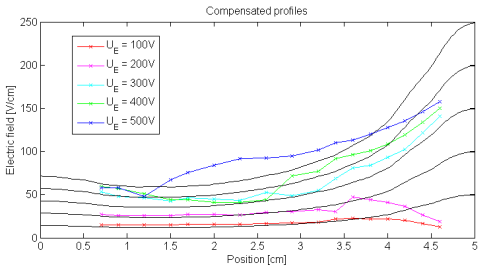

Figure 4.2 – Reconstruction by the algorithm for static fields in vacuum

The obvious problem with inverting the geometrical saturation functions to obtain information about the electric field from experimental data is that they are not one-to-one. Therefore one must manually separate the recorded points of data into two groups, one for which the left part of the curve (before saturation) is used and one for which the right part (after saturation) is used. This is readily done by taking a point for which the recorded profile data reaches a maximum as a dividing point. All points on one side of the maximum are considered 'before saturation' and the ones on the other side 'after saturation'. The electric field is calculated for every point by inverting the appropriate part of the saturation function. Results are shown for various voltage values in Fig. 4.2.

Using the program *Finite Element Method Magnetics*[5], the field profiles have also been numerically calculated with a finite element method (black continuous lines in the background

of Fig. 4.2). Sufficiently far away from the biased plate, the agreement between measured data and numerical results is in most cases very good. The difficulties with reconstructing the electric field close to the biased plate in these cases are probably due to large variations in z_0 because the geometrical saturation is different close to the plates than far away from them. There might be also an inadequate plate influence compensation. But both these problems are very specific to our machine and does not present themselves in a situation where our method is intended to be applied. In conclusion, they can be disregarded for the purpose of showing the prospective usefulness of the method.

5. Conclusions: Prospects and limitations of our method, possible continuations

As described in the previous sections, the method of measuring electric fields by use of a metastable atomic hydrogen beam has the potential of becoming useful in a number of situations. It can be implemented to non-intrusively probe both static and sinusoidally time varying electric fields in vacuum and in plasma discharges with low enough values of pressure and discharge current. Studying the exact limitations of the region of plasma parameters within which the method can be used, as well as optimizing it for practical use in a general plasma device are two topics for continued research. An upper limit to some parameters is set by the fact that in a very hot and/or dense plasma, a hydrogen atom beam will become completely ionized on time scales faster than those related to Stark mixing or the spontaneous decay of $2p_{1/2}$. Therefore, we picture the primary usage areas to be the edge plasma of fusion devices and cold laboratory plasmas in general ($T_e \lesssim 10$ eV).

Acknowledgments

Parts of this article are extracted from Ref. [2].

References

[1] W.E. Lamb and R.C. Retherford, *Fine Structure of the Hydrogen Atom by a Microwave Method*, Phys. Rev. **72**, 241 (1947)

[2] P. Ström, *Measurements of electric fields in a plasma by Stark mixing induced Lyman-α radiation*, http://urn.kb.se/resolve?urn=urn%3Anbn%3Ase%3Auu%3Adiva-206123 (2013)

[3] M. Carrère, L. Chérigier, C. Arnas-Capeau, G. Bachet and F. Doveil, *Steady state behavior of a multipolar plasma device*, Rev. Scient. Instr., **67**, 4124 (1996)

[4] M. Bacal and W. Reichelt, *Metal vapor confinement in vacuum*, Rev. Sci. Instrum. 45, 769 (1974)

[5] Homepage of Finite Element Method Magnetics, visited 30/4 - 2013 ; http://www.femm.info/wiki/HomePage